HardwareX 12 (2022) e00360

Contents lists available at ScienceDirect

HardwareX

journal homepage: www.elsevier.com/locate/ohx

Hardware Article

MADV-DAQ: Multi-channel Arduino-based differential voltage data acquisition system for remote strain measurement applications

Hendrik Louw, André Broekman *, Elsabé Kearsley

Department of Civil Engineering, University of Pretoria, Pretoria, South Africa

ARTICLE INFO

Article history:
Received 14 June 2022
Received in revised form 28 August 2022
Accepted 18 September 2022

Keywords:
Multi-channel data acquisition system
Remote strain measurements
Structural health monitoring
Soil-structure interaction
Onshore wind turbines
Arduino

ABSTRACT

Wind turbine power generation, both onshore and offshore, has gained significant popularity over the past few decades. However, the design of a turbine's foundation, capable of supporting a tall structure subject to large horizontal forces, remains challenging. Complex wind loading and intricate soil-structure interaction between the foundation and the supporting soil requires consideration. Although commercial structural health monitoring (SHM) systems provide several advantages, they remain cost prohibitive. This paper demonstrates the development, testing, fabrication, installation and validation of a low-cost, multi-channel, Arduino-based differential voltage data acquisition system (MADV-DAQ) suitable for remote, battery powered measurements of multiple Wheatstone bridge-based (strain) sensors. The instrumented wind turbine (120 m high, 3.45 MW generation capacity) forms part of a newly constructed onshore wind farm in South Africa. The developed MADV-DAQ system proved valuable in measuring strains associated with the wind turbine tower, quantifying the true magnitude of the loads being transferred to the underlying foundation. MADV-DAQ was designed to relay the real-time measurements to two, independent cloud platforms for aggregation, visualization and subsequent analysis. MADV-DAQ was purposefully designed as a universal data acquisition system, compatible with any Wheatstone bridge-based sensor design, including strain gauges, tensiometer and similar MEMS-based sensors.

Specifications table

Hardware name	MADV-DAQ (multi-channel Arduino-based differential voltage data acquisition system for remote strain measurement applications)
Subject area	Engineering and materials science
Hardware type	Measuring physical properties and in-lab sensors Electrical engineering and computer science
Closest commercial analog	DataTaker, HBM QuantumX series, MOVE analog LoRaWAN node
Open source license	Creative Commons Attribution-ShareAlike
Cost of hardware	$400 USD
Source file repository	https://doi.org/10.17605/OSF.IO/TK8Z9

* Corresponding author.
E-mail addresses: hendrik.louw@tuks.co.za (H. Louw), u13025059@tuks.co.za (A. Broekman), elsabe.kearsley@up.ac.za (E. Kearsley).
@@BroekmanAndre (A. Broekman)

https://doi.org/10.1016/j.ohx.2022.e00360
2468-0672/

1. Hardware in context

Wind turbine power generation, both onshore and offshore, has gained significant popularity over the past few decades as an option for cleaner energy production amidst growing climate change concerns. South Africa has over recent years invested heavily in onshore wind turbine technologies, not only to satisfy the ever-growing demand for electricity caused by a growing population, but also to reduce its carbon footprint as a large portion of electricity is still generated from fossil fuels. The current focus with new wind farm construction is on taller wind towers, allowing for the same generation capacity from fewer wind turbines. However, this poses a significant challenge to design foundations capable of supporting these taller structures, having to not only consider the complex dynamic loading caused by the wind, with the effect amplified for taller wind turbines, but also the intricate soil-structure interaction between the foundation and the supporting soil.

Structural health monitoring (SHM) is a powerful tool, enabling engineers to improve their current understanding of how any infrastructure behaves under working loads and changing environmental conditions, allowing for more economic and sustainable designs in future. Alternatively, SHM not only allows stakeholders of the infrastructure to monitor the response of their infrastructure under serviceability load conditions, but also the prediction of the response over the lifespan of that infrastructure. As a result, the useful service life could potentially be extended by means of maintenance and rehabilitation [1]. Although SHM systems provides several advantages, it is typically neglected when constructing new infrastructure due to the high costs associated with the installation of sensors and long-term monitoring systems. However, Internet-of-Things technologies (e.g., LoRaWAN) is rapidly addressing this limitation [2,3].

Limited research has been conducted in the past [4–8] for SHM of onshore wind turbines and wind turbine foundations; both low-cost wireless sensors and technologies, and commercially available options have, however, proved successful. Following recent examples from the University of Pretoria, whereby low-cost data acquisition systems (DAQ) [9,10] and a closed-loop controller for geotechnical centrifuge modelling [11] were successfully developed, a low-cost DAQ for long-term wind turbine and wind turbine foundation monitoring was explored. Commercial DAQ hardware and software (Fig. 1), whilst providing robust performance and feature rich configurations and characteristics, are both prohibitively expensive to earmark for long-term monitoring and require manual intervention where computers are involved in an environment characterized by intermittent power availability and network connectivity.

This paper demonstrates the development, testing, fabrication, installation, and validation of a low-cost, multi-channel, Arduino-based differential voltage data acquisition system (MADV-DAQ) suitable for remote, battery powered measure-

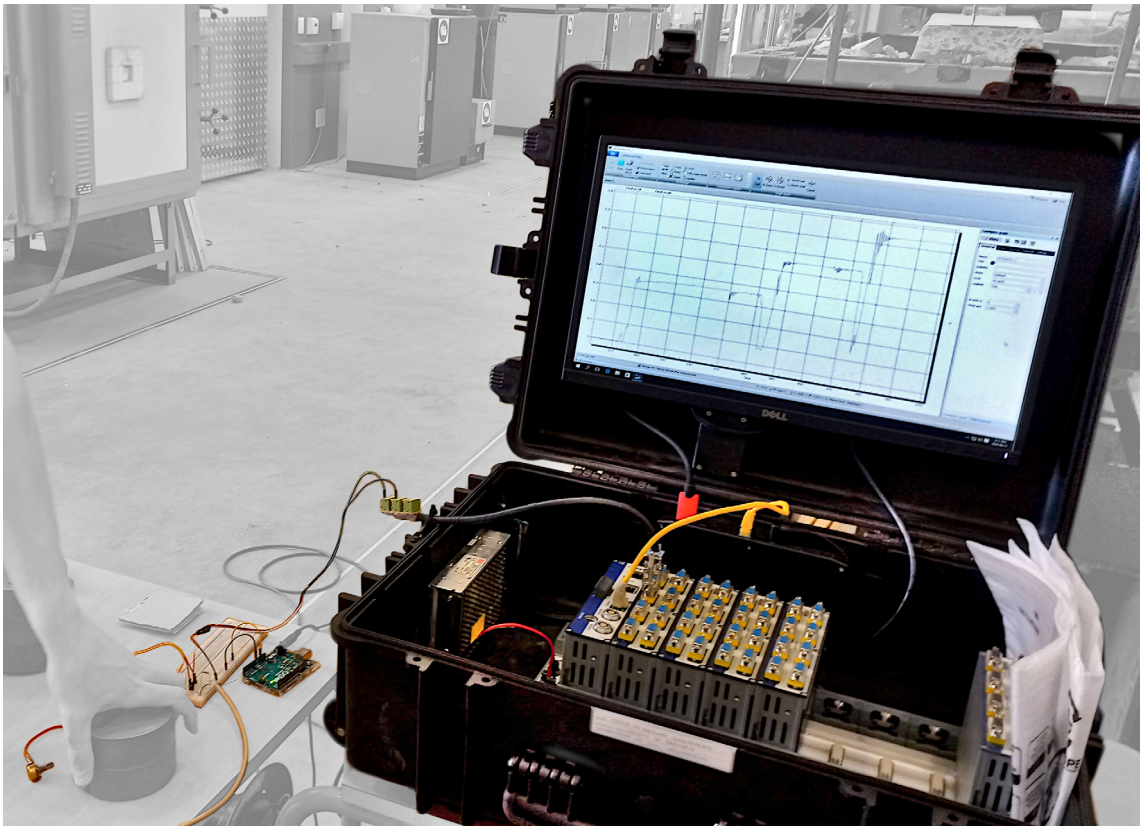

Fig. 1. Example of a commercial data acquisition system used in a civil engineering laboratory.

Fig. 2. Photograph of a wind turbine on a wind farm in South Africa.

ments of multiple Wheatstone bridge-based sensors, primarily strain gauges. Both vibrating wire strain gauges (VWSG) and conventional strain gauges were installed on both a wind turbine tower and its supporting reinforced-concrete piled-raft foundation with the turbine having a height of about 120 m (Fig. 2). This allowed for the soil-structure interaction mechanisms between the foundation of a wind turbine, subjected to large dynamic loadings, and its supporting soil, to be investigated through SHM. The increased prevalence of wind turbine technology as a cleaner avenue for generating electrical power necessitates detailed research of the structural dynamics, balancing the need for safe design practices whilst minimizing the resources required to address the design criteria. MADV–DAQ follows from a successful development history within the Department of Civil Engineering at the [12] of low-cost research hardware to address a diverse array of practical applications and use-cases [13,14].

2. Hardware description

Recently, the need for a multi-channel (minimum of twelve) DAQ capable of recording and relaying strain (differential voltage) measurements from a remotely located wind farm, was identified. Due to funding constraints and extensive experience with the Arduino microcontroller platform, this low-cost avenue was explored to realize an economical solution with a minimum amount of development time. Hence the MADV-DAQ acronym was derived: *Multi-Channel Arduino-based Differential Voltage Data Acquisition System*. Commercial solutions were available but remained cost-prohibitive for the desired number of strain measurements required. Additionally, collated data was restricted to proprietary data platforms that could not be integrated with existing data aggregation systems under active development within the research group. The design specifications of the DAQ, suited to address the project requirements, are summarized below:

- Remote control of the DAQ over the internet (cellular network connectivity).
- Support for multiple, accurate, high-resolution differential voltage measurements.
- Integration of measurements with existing data platforms alongside localized, non-volatile storage.
- Continuous, autonomous operation over a two-year period (estimated duration of the project).
- Backup power supply for a continuous, 7-day operational period.
- Optional high-frequency strain measurements to investigate dynamic behavior of a structure.

From design specifications list, MADV-DAQ was designed as a hybrid system, featuring an Arduino microcontroller as the primary DAQ, with a secondary Raspberry Pi relaying the information to two independent data platforms for long-term storage and analysis (Fig. 3 and Fig. 4). For the intended application, a permanent electrical power supply was available, eliminating the need for low-power IoT (Internet of Things) orientated communications technologies such as [15] and LoRa [16]. Instead, a 4G LTE router with a dedicated Wi-Fi access point (AP) could be deployed and paired with a low-cost, low-power Raspberry Pi platform to parse and relay the measurements to a dedicated cloud platform using a Python implementation. This design also allows for remote access and reconfiguration of the software script if desired. The microcontroller still serves as the primary sensor platform to store data on non-volatile storage (SD card) in the event of a communications failure. The differential voltage measurements associated with the strain gauges are quantified using a low-cost, high-resolution analog-to-digital (ADC) converter [17]. The Arduino was selected for its compatibility with the ADC (I2C interface), SD card (SPI interface), battery-power backup and connectivity interface (USB) with the Raspberry Pi. The Raspberry Pi in turn provides

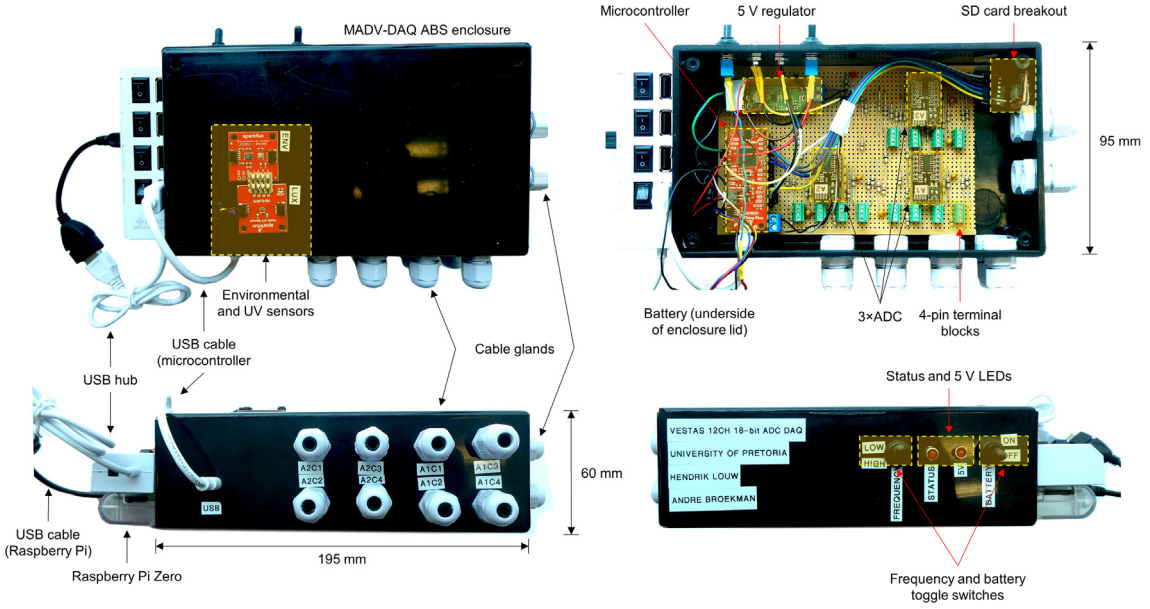

Fig. 3. Plan and elevation view of MADV-DAQ, including the electronic components.

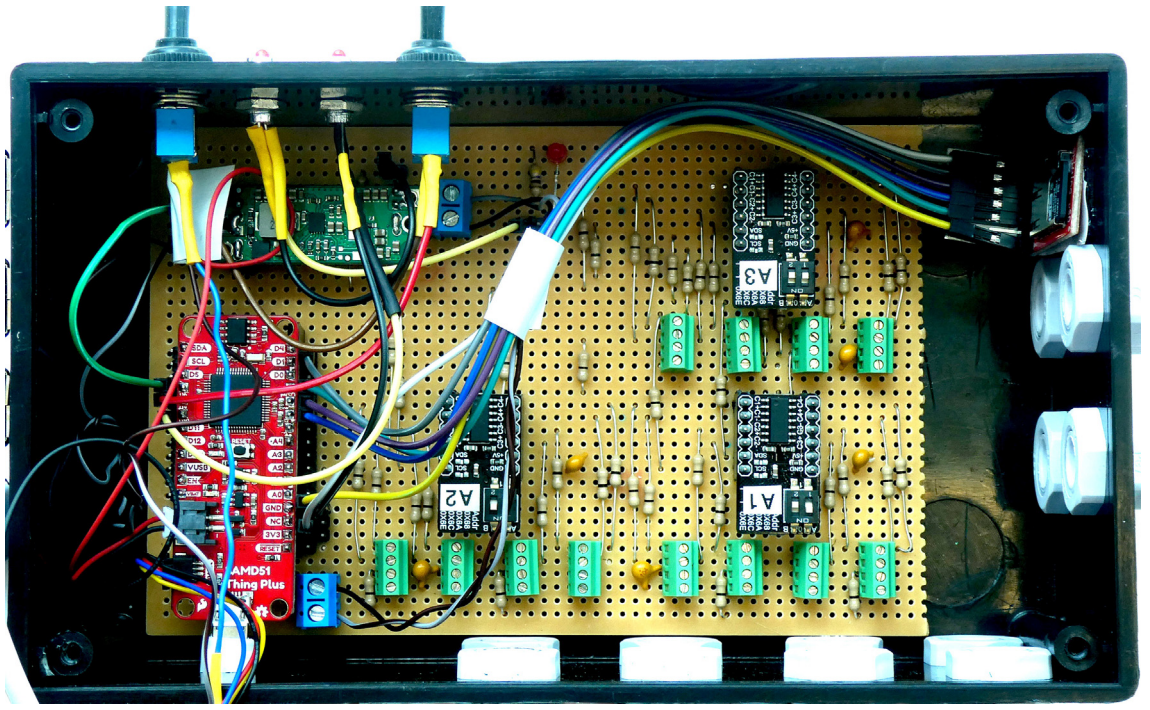

Fig. 4. Plan view of the electronic components and populated veroboard.

the cheapest solution to deploy a remotely accessible, internet connected, programmable computer interface to relay the information from the Arduino to the data platform(s) of choice. Auxiliary environmental sensors record the local environmental parameters in tandem with the differential voltage measurements. Fig. 5 summarizes the functional design MADV-DAQ and associated data services. The MADV-DAQ demonstrates advantages that could benefit the community and researchers alike:

• General-purpose quantification (measurement) of Wheatstone bridge-based sensors, ranging from strain gauges to tensiometers (MEMS-based devices) that are installed in a wide range of applications and environments. These sensors typically

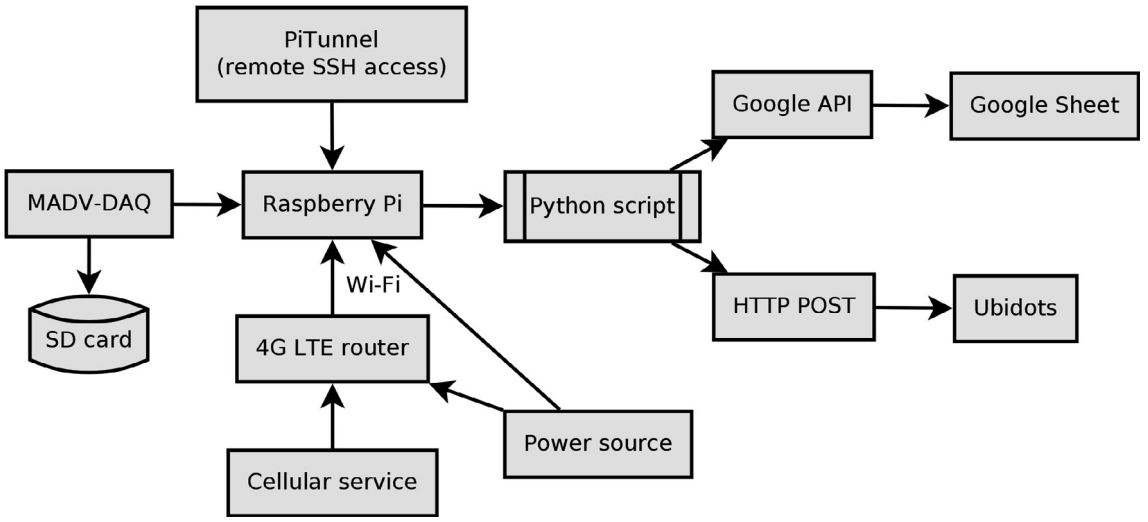

Fig. 5. Description of the primary hardware and software elements of MADV-DAQ.

accommodate a wide range of excitation voltages, producing a proportional differential voltage that is correlated (calibrated) to the physical response under study. The purely analog sensing mechanism is agnostic to the sensing implementation of the DAQ, requiring no additions or modifications to the platform.

• Improved understanding of complex, long-term soil-structure interaction associated with wind turbines that are deployed across the world as a renewable energy source. These range from dynamic effects associated with the turbine (>1 Hz) and structural response (<1 Hz), to seasonal variations over the course of a year. MADV-DAQ hardware specifications supports all of these measurement regimes, only requiring the corresponding firmware implementation to execute to the user or project requirements.

• Serving as a stand-alone, battery-powered DAQ that can be adapted for wireless monitoring applications or general laboratory work where hardware is in limited supply for a large student or researcher population. The microcontroller could be substituted for hardware integrating IoT-based capabilities for field work applications. Additionally, the simplified electronic design is ideal for duplicating multiple MADV-DAQs with limited training required.

• Serving as a general purposes sensors platform where additional sensors could be added (i.e., SDI12, a serial data interface and communication standard). This is only limited by the physical interfaces supported by the microcontroller. Firmware support in the form of open-source libraries provide out-of-the-box support to interface digital sensors such as SDI12 sensors that are employed for geotechnical investigations [9].

3. Design files summary

The complete list of files is summarized in Table 1. These files provide the necessary information and software to duplicate and implement an equivalent MADV-DAQ. The files are accessible from the Open Science Framework source file repository linked together with this manuscript. Fig. 6 illustrates an overview of the electronic design of the DAQ [18].

MADVDAQ.ino: Arduino sketch (firmware) for the SparkFun Thing Plus microcontroller, executing the functions as described for measuring, parsing, storing and transmitting differential voltage and environmental data.

Libraries.zip: Archive containing all of the necessary libraries to compile the *MADV-DAQ.ino* Arduino sketch.

MADVDAQ_design.sch: ExpressSCH electronic schematic file detailing the hardware configuration of the MADV-DAQ.

MADVDAQ_design.pdf: PDF version of the ExpressSCH electronic schematic file.

Table 1
Complete list of design files.

Design file name	File type	Open source license	Location of the file
MADVDAQ.ino	Arduino sketch (.ino)	CC BY 4.0	Source file repository (*Arduino* folder)
Libraries.zip	Archive (.zip)	CC BY 4.0	Source file repository (*Arduino* folder)
MADVDAQ_design.sch	ExpressSCH (.sch)	CC BY 4.0	Source file repository (*Schematic* folder)
MADVDAQ_design.pdf	Portable Document Format (.pdf)	CC BY 4.0	Source file repository (*Schematic* folder)
main.py	Python script (.py)	CC BY 4.0	Source file repository (*Python* folder)
MADVDAQ_vero.diy	DIY Layout (.sch)	CC BY 4.0	Source file repository (*Veroboard* folder)
MADVDAQ_vero.pdf	Portable Document Format (.pdf)	CC BY 4.0	Source file repository (*Veroboard* folder)

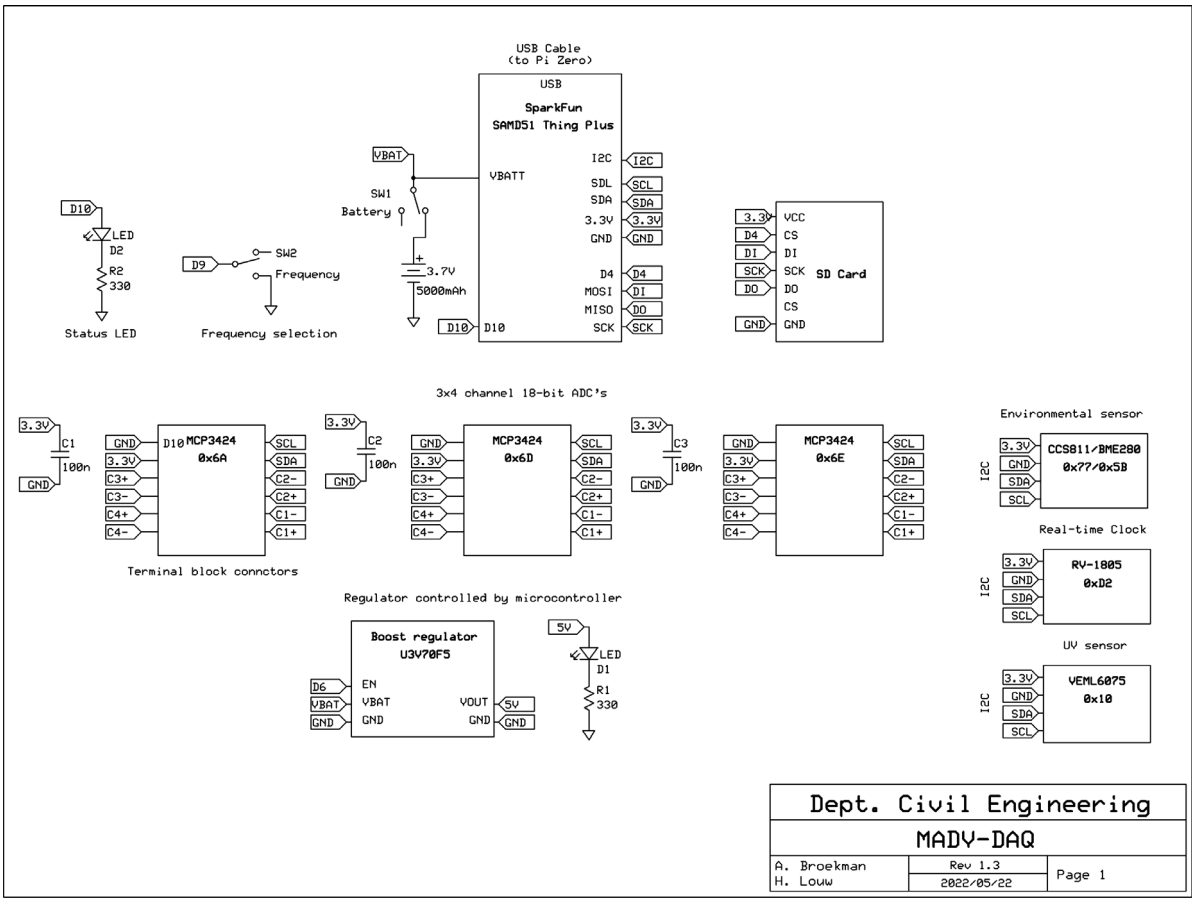

Fig. 6. Electronic design overview of the MADV-DAQ.

main.py: The primary control script written in Python running on the Raspberry Pi. Serial data is received from the Arduino, parsed, and sent to the cloud services for storage.

MADVDAQ_vero.sch: DIY Layout file detailing the veroboard layout / design (Fig. 4).

MADVDAQ_vero.pdf: PDF version of the *MADVDAQ_vero.sch* design.

4. Bill of materials summary

The complete bill of materials (BOM) for replicating the MADV-DAQ is listed in Table 2. The components are general purpose electronics that can be sourced from various local and international suppliers.

5. Build instructions

The summarized building instructions for replicating the MADV-DAQ is summarized for each of the primary components, namely the microcontroller, ADC, voltage regulation, veroboard integration and power design considerations.

5.1. Microcontroller

The [19] SAMD51 Thing Plus microcontroller was selected for its support for a Lithium Polymer (LiPo) battery, Qwiic connector, fast processor (120 MHz), ample memory capacity (1 MB flash memory, 256 KB static random access memory (SRAM) with error correction) and 600 mA 3.3 V regulator. The firmware was developed using the ubiquitous [20].

5.2. Analog-to-digital converter (ADC)

The MCP3424 [17], 4-channel, 18-bit ADC was selected for its low-cost and versatility. The integrated programmable gain amplifier (PGA) is defined in the firmware, adjusting the full-scale (FS) of the ADC in discrete steps from ± 0.256 V to ± 4.

Table 2
MADV-DAQ Bill of Materials.

Designator	Component	Number	Cost per unit - currency	Total cost - currency	Source of Materials	Material type
MADV-DAQ	Enclosure (ABS, 195 mm × 110 mm × 60 mm)	1	$7.13 USD	$7.13 USD	https://www.robotics.org.za/P148	Other
	Microcontroller (SparkFun Thing Plus - SAMD51)	1	$29.84 USD	$29.84 USD	https://www.robotics.org.za/DEV-14713	Other
	Real time clock (SparkFun Qwiic RV-1805)	1	$21.03 USD	$21.03 USD	https://www.robotics.org.za/BOB-14558	Other
	UV sensor (SparkFun Qwiic - VEML6075)	1	$8.73 USD	$8.73 USD	https://www.robotics.org.za/SPX-14748	Other
	Environment combo breakout (SparkFun Qwiic - SEN-14348)	1	$55.03	$55.03	https://www.robotics.org.za/SEN-14348	Other
	Micro SD card breakout (SparkFun - BOB-00544)	1	$9.46	$9.46	https://www.robotics.org.za/BOB-00544	Other
ADC	MCP3424 ADC (4-channel, 18-bit)	3	$17.10	$51.31 USD	https://www.robotics.org.za/DFR0316	Other
	Micro SD card (16 GB, class 10)	1	$6.48	$6.48 USD	https://www.robotics.org.za/MSD16	Other
	Battery (LiPo, 5000 mAh, 3.7 V)	1	$13.76	$13.76 USD	https://www.robotics.org.za/105570	Other
	Voltage regulator (Pololu 5V8A U3V70F5, step-up)	1	$12.96	$12.96 USD	https://www.robotics.org.za/2891	Other
	Veroboard (100 mm × 150 mm)	1	$2.77	$2.77 USD	https://www.robotics.org.za/VERO100150	Other
	SIL male header (40 Way, 2.54 mm, 10-pack)	1	$1.09	$1.09 USD	https://www.robotics.org.za/HMST-40-TH254	Other
	SIL female header (15-pin, 2.54 mm, 10-pack)	1	$0.87	$0.87 USD	https://www.robotics.org.za/HFST-40-TH254	Other
	Terminal block (screw, 4-pin, 2.54 mm, 10-pack)	1	$3.93	$3.93 USD	https://www.robotics.org.za/KF120-4P	Other
	Terminal block (screw, 2-pin, 2.54 mm, 10-pack)	1	$1.02	$1.02 USD	https://www.robotics.org.za/KF301-2P	Other
	Qwiic Connect Cable (male-male, 50 mm)	1	$1.46	$1.46 USD	https://www.robotics.org.za/PRT-14426	Other
	Qwiic Cable (breadboard jumper, 4-pin)	1	$2.04	$2.04 USD	https://www.robotics.org.za/PRT-14425	Other
	Toggle Switch (2-pole, splash proof, 4-pack)	1	$2.11	$2.11 USD	https://www.robotics.org.za/MTS-101-COVER	Other
	Resistors (0 O, 100-pack)	1	$7.54	$7.54 USD	https://za.rs-online.com/web/p/through-hole-resistors/1251170	Other
	Resistors (330 O, 10-pack)	1	$2.64	$2.64 USD	https://za.rs-online.com/web/p/through-hole-resistors/7077622	Other
	LED (5 mm, red, 10-pack)	1	$0.73	$0.73 USD	https://www.robotics.org.za/LED-RED-5MM	Other
	Decoupling capacitors (100 nF)	1	$0.73	$0.73 USD	https://www.robotics.org.za/100NF-10	Other
	Cable glands (5-pack)	3	$3.88	$11.65 USD	https://za.rs-online.com/web/p/cable-glands/8229644	Other
Raspberry Pi	Raspberry Pi Zero W	1	$29.04	$29.04 USD	https://www.robotics.org.za/PIZERO-WH	Other
	Raspberry Pi Zero enclosure (ABS, clear)	1	$2.11	$2.11 USD	https://www.robotics.org.za/PIZ-ABS-CLR	Other
	USB hub (4-port)	1	$4.51	$4.51 USD	https://www.robotics.org.za/USBHUB4	Other
	Mini HDMI to HDMI female Cable	1	$2.47	$2.47 USD	https://www.robotics.org.za/HDMI-HDMI-MINI	Other
	Power supply (3-port 5V3A)	1	$7.72	$7.72 USD	https://www.robotics.org.za/5V3A-DIS	Other
	Micro USB to USB Cable – 30 cm	1	$1.46	$1.46 USD	https://www.robotics.org.za/MUSB-USB-30CM	Other
	Micro SD card (16 GB, class 10)	1	$6.48	$6.48 USD	https://www.robotics.org.za/MSD16	Other
4G LTE router	4G LTE Router (TP-LINK MR100 Wireless 300 Mbps N)	1	$73.35	$73.35 USD	https://www.takealot.com/tp-link-mr6400-300mbps-wireless-n-4g-lte-router/PLID47195277	Other
	SIM card + 200 MB data plan (12 months)	1	$22.78 USD	$22.78 USD	Local cellular service provider (MTN for MADV-DAQ)	Other
	Total cost for MADV-DAQ	1		$404.23 USD		Other

096 V. From experience, Wheatstone bridge implementations, for the purposes of measuring the strain of concrete and steel structures, will seldom exceed 20 mV. Thus, the FS of the ADC was configured as ± 0.256 V, maximizing the effective resolution (0.98 μV/digit). Furthermore, the maximum ADC resolution of 18-bits was selected for increased accuracy and resolution. The 18-bit configuration necessitates approximately-one second to measure all four differential channels, or three seconds for all twelve channels that are included in the design. The ADC can be assigned up to four different I2C addresses, eliminating the need for an auxiliary multiplexer (Fig. 7). A 4-pin terminal connector is provided for each channel, reducing the probability of wiring mistakes and avoiding the need to connect multiple power conductors to a single physical interface. The Wheatstone bridge is powered by a digitally controlled, high current 5 V regulator (refer to Section 5.6) that exhibits minimal ripple (Fig. 8). The ADC in turn amplifies and digitizes the differential voltage measurement. The ADC's integrated PGA removes the need to provide an external reference voltage altogether, with the regulator controlled by the Arduino to minimize the power consumption.

The performance of an identical ADC was demonstrated by both Basson et al. [9] for the purposes of measuring soil suction in a tailings storage facility (TSF) and Broekman et al. [11] for closed-loop control of a geotechnical centrifuge. Basson et al. compared the measurements from the Wheatstone-bridge sensors acquired by the low-cost ADC against a commercial DAQ, achieving excellent accuracy and linearity; based on these results, and additional resource constraints owing to the remote installation location of MADV-DAQ, no comparative strain measurements were performed.

5.3. Auxiliary sensors

Auxiliary sensors are included to measure the environmental parameters in the vicinity of MADV-DAQ as well as keeping track of the time: an environmental combo sensor (CCS811 / BME280 [21]) measuring temperature (−40 °C – 85 °C; ±1.0 °C) and relative humidity (0 %RH – 100 %RH; ±3 %RH), UV sensor (VEML6075 [22]) (0 – 13 index) and accurate (±2.0 ppm) real-time clock (RV 1805 [23]). For certain scenarios, including the application where the MADV-DAQ was deployed, quarter Wheatstone bridge configurations were required (one active strain gauge together with three passive precision resistors). The temperature variations induce a drift (bias) in the resulting measurements that can be readily removed, provided the local environmental temperature is measured. The change in barometric air pressure is also recorded to verify the correlation

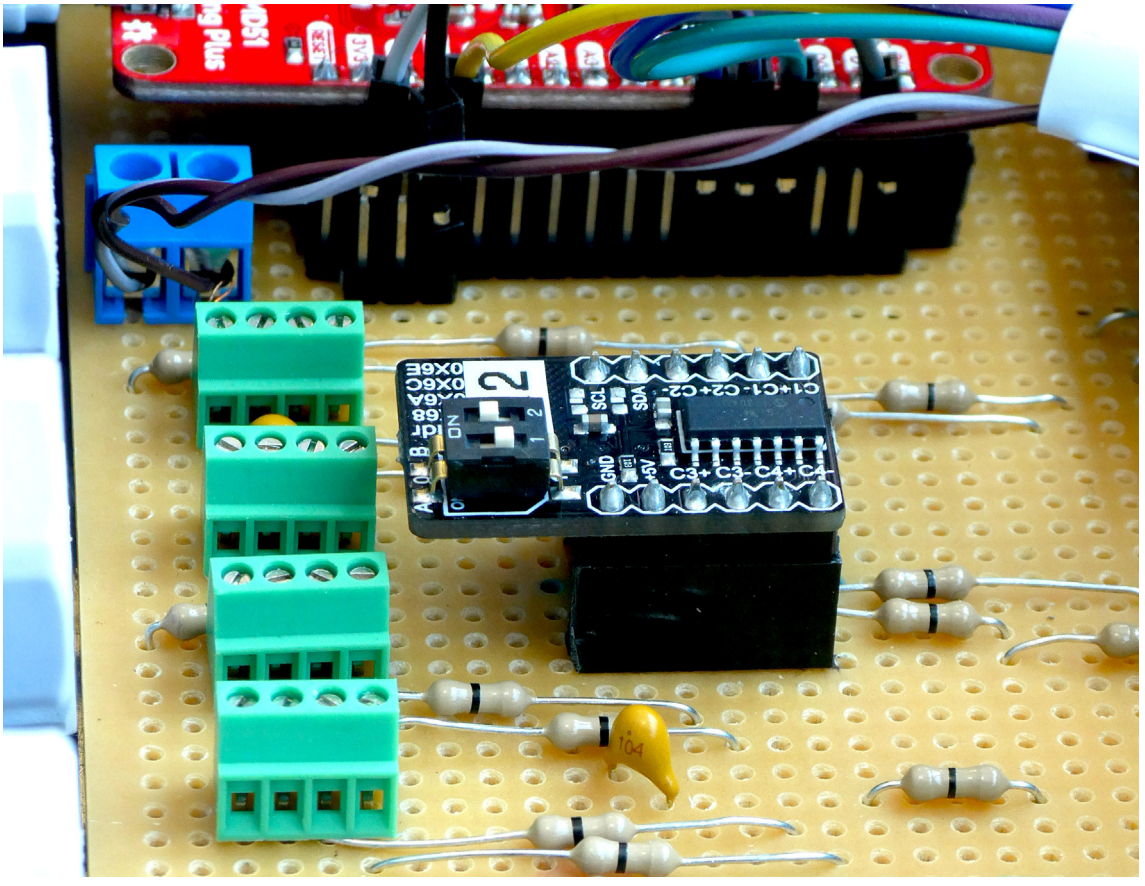

Fig. 7. Close-up view of the hardware implementation of the MADV-DAQ.

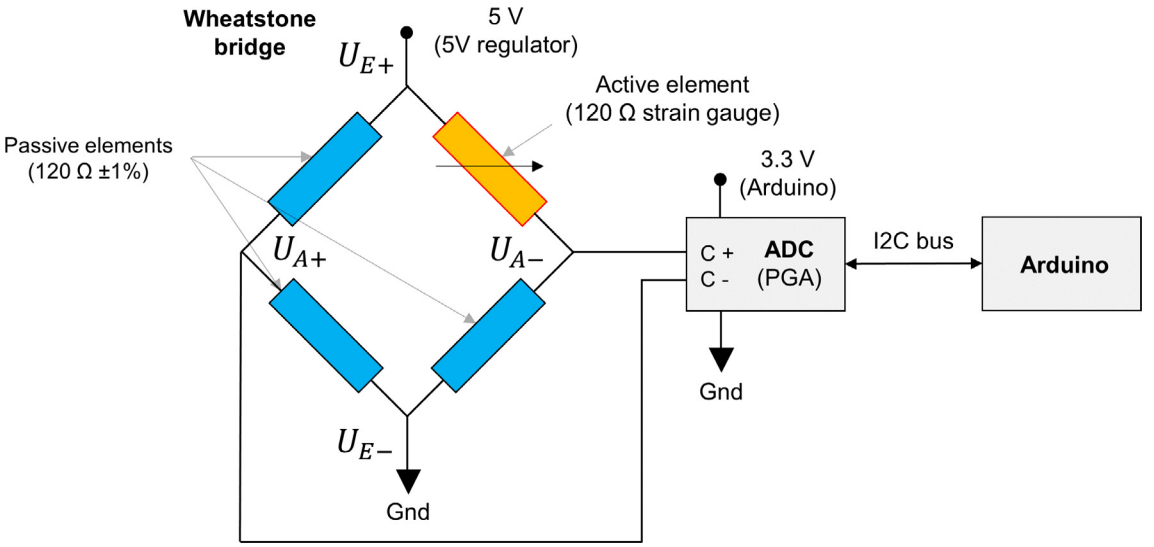

Fig. 8. Simplified schematic illustrating the integration between the Wheatstone bridge, ADC and Arduino.

between localized measurements and those of third-party weather stations (refer to operation instructions). The real-time clock (RTC) provides accurate, long-term time measurements; this is necessitated for data stored on the local SD card (non-volatile storage). Data stored on cloud platforms are automatically timestamped upon ingestion, reducing the size and complexity of the payload transmission. To improve the reliability of the I2C bus, the pull-up resistors were removed from the BME280/CS811 combo and UV light sensor with a crafting knife.

5.4. Veroboard integration

Fig. 9 illustrates the [24] veroboard design integrating all the electronic components. Veroboard was preferred over a PCB (printed circuit board) owning to the associated costs and flexibility to alter the prototype as required. The veroboard was cut to size, limited only by the dimensions of the enclosure, using a crafting knife. The conductive copper tracks were separated using a drill press and 4 mm drill bit. Zero-ohm (0 Ω) resistors, functioning as orthogonal interconnects, saved a significant amount of time compared to stripping and soldering copper (wire) conductors; for clarity, the interconnects are colour coded according to their function. Components were then soldered, starting with the lowest elevation components

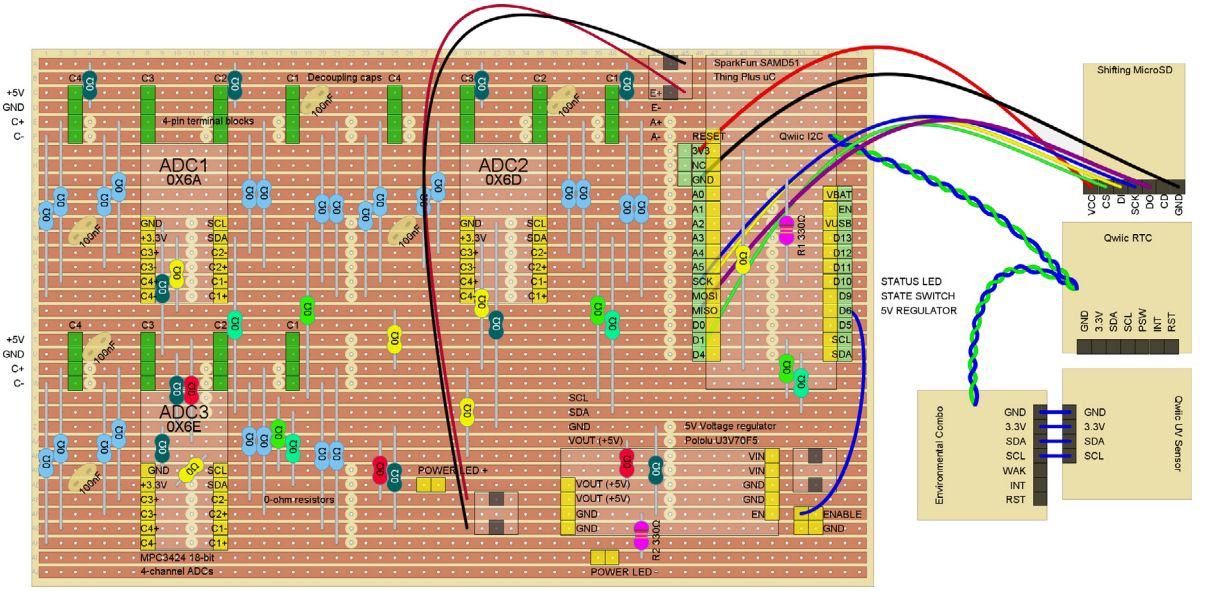

Fig. 9. Veroboard hardware design of the MADV-DAQ.

(resistors, capacitors, and headers). Female headers with a 0.1″ pin spacing on the veroboard match the pin allocation of the ADCs, voltage regulator and microcontroller (0.1″ male headers). Decoupling capacitors (100 nF) are installed in the vicinity of the power leads for each of the ADCs and on the power rails to suppress high frequency voltage variations associated with the voltage regulator's power cycling. Male headers are provided for the status LED and frequency selection switch. Jumper wires were used to connect the SD card reader to the microcontroller. SparkFun's Qwiic connect system connects the various breakout sensors.

5.5. Enclosure

The ABS enclosure measures 195 mm × 110 mm × 60 mm. The battery and sensors are fixed on the lid (Fig. 4). Cable glands were installed for the 12 cables to prevent accidental tearing or shearing of the connectors if a cable is tensioned. The diameter of the holes was small enough such that a standard drill press was used for their fabrication. No consideration was given for water- or dustproofing as the intended installation applications are for covered areas.

5.6. Power design

The 5 000 mAh LiPo battery supplies a nominal output voltage of 3.7 V that varies from 4.15 V when fully charged, down to 3.3 V whereupon the built-in protection circuitry disables the battery. The 5 V voltage supplied by the regulator (Pololu U3V70F5) is within 10 mV of the target value [9]. The current capacity of the voltage regulator was intentionally oversized to reduce any voltage ripple and variation. The Wheatstone bridge, consisting of four 120 O active and passive elements, requires 42 mA with an excitation voltage of 5 V. For the desired 12-channel design, the total current consumption is approximately 500 mA (2.5 W). The regulator is controlled by the microcontroller to cycle power only when measurements are acquired. The microcontroller and sensors, when idle, consumed 20 mA of current. Table 3 summarizes the expected runtime performance of MADV-DAQ. For a 5-minute logging cycle, an approximate runtime of 7 days can be expected, compared to 6.7 h for continuous logging (refer to operation instructions) of the strain gauges.

5.7. Networking

Internet connectivity was provided for the Raspberry Pi Zero in the form of a Wi-Fi AP using a 4G LTE router (Table 2). A SIM card with a small data package (250 MB per month) was acquired, operating on a local cellular provider for network connectivity. The performance of the network carrier was verified on site prior to the hardware installation.

Table 3
Summary of the power consumption of MADV-DAQ.

Parameter	Value	Unit
Nominal voltage	3.7	V
Capacity	5 000	mAh
Power efficiency	0.9	–
Number of Wheatstone bridges	12	–
Effective bridge resistance	120	Ω
Excitation voltage	5	V
Powered phase (microcontroller)	3	s
Sleep phase (microcontroller)	300	s
Energy available		
Total energy	18.5	Wh
Usable energy	16.65	Wh
Sleep Phase (microcontroller)		
Total current	20×10^{-3}	A
Excitation Voltage	3.7	V
Total power	74×10^{-3}	W
Total on-time	83.3×10^{-3}	h
Energy per cycle	6.17×10^{-3}	Wh
Powered phase (microcontroller + strain gauges)		
Current per bridge	41.7×10^{-3}	A
Total current	0.5	A
Total power	2.5	W
Total on-time	833×10^{-6}	h
Energy per cycle	2.083×10^{-6}	Wh
Combined power and sleep phases		
Total energy of powered and sleep phases	8.25×10^{-3}	Wh
Total number of DAQ cycles	2018	–
Total powered time (minutes)	10 090	m
Total powered time (hours)	168	h
Total powered time (days)	7.01	d
High frequency logging time (hours)	6.66	h

5.8. Raspberry Pi

The Raspberry Pi Zero is installed in plastic enclosure that is affixed to the side of MADV-DAQ's enclosure with double-sided tape. The Raspberry Pi's SD card, preloaded with the latest edition of Raspberry OS [25], is installed in the corresponding SD card socket. The USB hub is also attached using the same method. A short USB (serial output) cable connects the microcontroller to one of the ports on the USB hub. The USB hub provides additional ports for connecting a keyboard and mouse as part of the software installation and configuration. If there is a power interruption (for the 4G LTE router and Raspberry Pi Zero), the MADV–DAQ will continue to acquire measurements, storing data on the SD card for later retrieval.

6. Operation instructions

The operation instructions are subdivided for both the Arduino and Raspberry Pi integration as the functionality of each is independent.

6.1. Arduino

The Arduino was programmed to operate in two complementary modes: low-frequency and high-frequency data acquisition. The mode is controlled by the toggle switch denoted *FREQUENCY* (Fig. 4). The low frequency mode samples all the auxiliary sensors and 12 ADC channels (18-bit, ±0.256 V) once, before writing the entry to the SD card (data.csv file) and sending the data over the serial output in parallel. This cycle is repeated indefinitely every 5 min and is the default operating mode.

The high frequency mode adds an additional function after the single measurement (low frequency modes) is completed. All the ADCs are reconfigured to a 14-bit resolution (maintaining a FS of ±0.256 V), allowing for continuous sampling (60 Hz) of the first channel of all three the ADCs for a 1-minute period. This is advantageous when measuring the dynamic strain response of the instrumented turbine tower. The high frequency data file is stored as a uniquely named UnixTime.csv CSV file. After the high-frequency data acquisition cycle has terminated, the loop restarts immediately with no rest period in between. At the start of every loop, the position of the frequency toggle switch is updated.

6.2. Raspberry Pi

The Raspberry Pi Zero was configured to automatically initiate the *main.py* Python script (available from the data repository) upon booting. The Python script automatically receives, decodes and uploads the measurements to both a spreadsheet (Google Sheets) and an integrated cloud aggregation service (HTTP integration). The *nohup* facility was used to initialize the script as a background process without requiring the user to start a new session. The full command, provided below, is appended to the */etc/rc.local* file that executes upon startup. The ampersand at the end of the command line ensures the script is initialized asynchronously. The COM post associated with the serial device (Arduino microcontroller) is determined automatically as this does not necessarily remain fixed.

```
nohup python3 -u /home/pi/Desktop/Python/main.py &
```

Due to the limited processing activity associated with the hardware and software of the Raspberry Pi Zero, a particular bug was encountered when generating RSA (Rivest–Shamir–Adleman) keys for communicating with Google's API (application interface). The lack of input events and limited processing occurring immediately after a power cycle is not sufficient for generating a sequence long enough for the RSA key as part of the cryptographic module. This was resolved with the addition of a 4-minute delay at the start of the script (prior to the import statements that would otherwise throw an assertion error). Remote access [26] was configured and tested successfully, allowing for reconfiguration of the Raspberry Pi over the duration of the project. The CLI (command line interface) further reduces the bandwidth requirements, limiting the data consumption and performance impact in the event of poor network coverage.

6.3. Google Sheets

Google Cloud provides an API to various services, allowing for automation of the data collection process. Google Sheets serves as a basic implementation to collect periodic information at no additional cost, given the low bandwidth requirements. The Python script automatically determines the applicable row to move the active cursor to, prior to adding all 19 measurements in the correct field for each data parameter received. An administrator account is created on the console, with the applicable spreadsheet configured to provide editor permissions for the account. The associated *key.json* credentials file contains the applicable private and public keys. Fig. 10 illustrates the hardware testing and verification of MADV-DAQ with the Raspberry Pi connected to a HDMI display: the laptop (Fig. 10, right) displays the Google Sheet with measurements populating the spreadsheet in real-time.

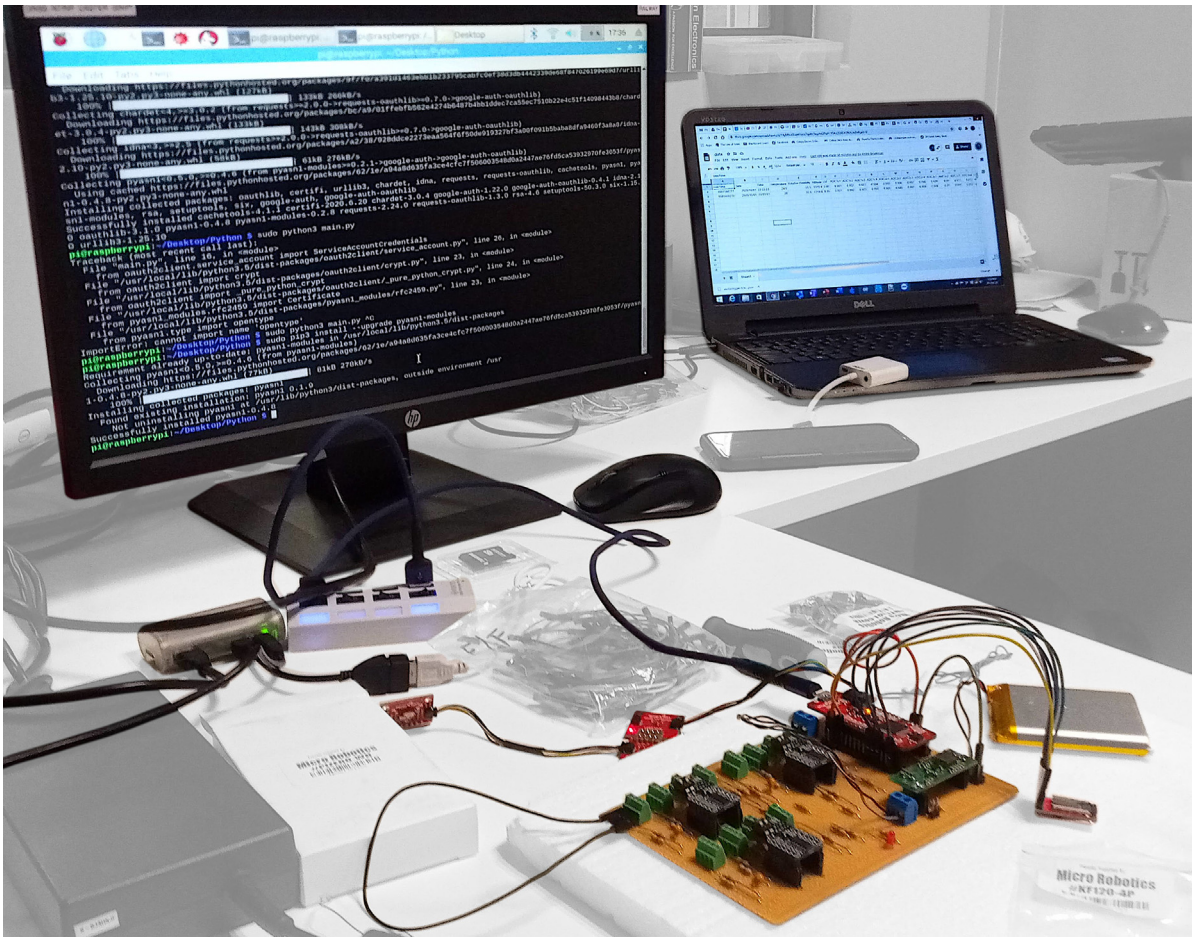

Fig. 10. Software installation (Raspberry Pi), debugging and hardware verification.

6.4. HTTP integration

Measurements were transmitted, in parallel to the Google Sheet implementation, to a dedicated cloud platform (Ubidots) developed primarily for the collection of LoRaWAN (Long-Range Wireless Access Network) IoT sensors [27]. The historical data record is visualized using a single dashboard with various widgets (Fig. 11). The cloud platform also integrates crowd-sourced data from publicly owned weather stations, eliminating potential cost and complexity associated with acquiring, installation and maintaining equivalent hardware for a remote project. Two weather stations from Weather Underground [28] and Open Weather Map [29], respectively, were specifically integrated with the target application of MADV-DAQ. Both these weather stations are in close proximity to the wind farm where the instrumentation was installed. Qualitative evaluations early in the project identified a strong correlation with the strain measurements and the direction and intensity of the wind, as was predicted from numerical models of the soil-structure interaction. This is explored in more detail in the next chapter.

7. Validation and characterization

With the focus of the research being to study the soil-structure interaction mechanisms involved with piled-raft foundations supporting wind turbines, a wind turbine tower and its supporting reinforced-concrete foundation was instrumented and monitored for an extended period, both during foundation construction and turbine installation, and after turbine commissioning. The instrumented wind turbine, with a hub height of about 120 m and generating capacity of 3.45 MW, is one of ten newly constructed wind turbines located on an onshore wind farm in South Africa.

For monitoring the foundation response, a total of 31 concrete embedment vibrating wire strain gauges (VWSG) were installed at various locations throughout the entire piled-raft foundation to investigate both the strains and temperatures within the piles and raft caused by the applied own weight, wind loading and changing environmental effects. These measurements were taken using a commercially available datalogger equipped to measure VWSGs (Fig. 12). To assess the

Fig. 11. MADV-DAQ dashboard hosted on the Ubidots cloud platform.

Fig. 12. MADV-DAQ and commercial datalogger installed inside the wind turbine tower.

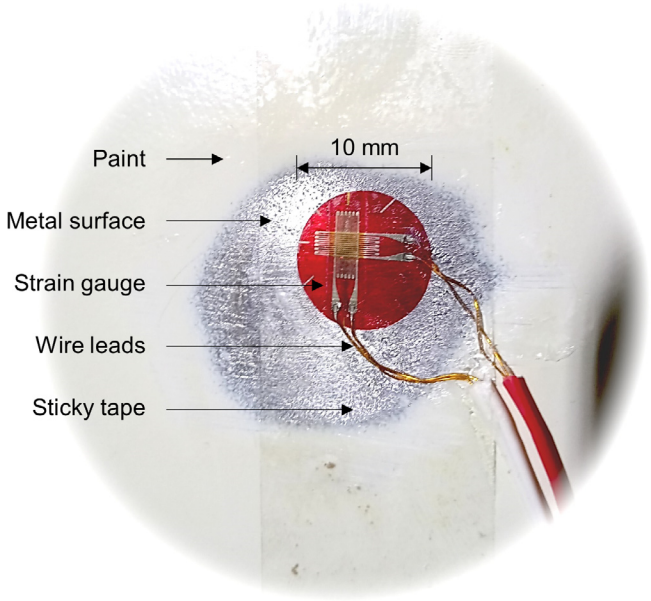

Fig. 13. Annotated strain gauge installation.

response of the turbine tower, and quantify the magnitude of loads and moments transferred to the underlying foundation, eight additional 120 Ohm quarter-Wheatstone bridge strain gauges (Fig. 13) were installed at the base of the wind turbine tower. This was monitored using the newly developed MADV-DAQ. These strain gauges were positioned at four locations along the inside circumference of the tower, 1.5 m from the base of the tower (Fig. 14a and Fig. 14b). At each position, two gauges were placed perpendicular to one another, with the vertical gauges measuring axial strain and horizontal gauges used for temperature compensation. Each location in Fig. 14b is labelled as indicated in black, with *T* referring to *Tower* and the accompanied number corresponding to the position of the strain gauges from the center of the turbine, relative to North expressed in degrees. By measuring quarter bridges, it is possible to distinguish between axial stresses (P/A) caused by the own weight of the turbine and bending stresses (M/Z) experienced by the tower caused by the wind.

Considering the response of the tower for the period of turbine installation (Fig. 15), an increase in axial stress in the base of the turbine tower was observed as the turbine was being constructed. Based on the total own weight and dimensions of the tower, theoretical calculations predicted the axial stress at the position of the strain gauges to be approximately 7.7 MPa, which is in good agreement with the measured axial stress data from the MADV-DAQ system. As expected, axial stress values remained constant thereafter. Bending stress experienced by at the base of the tower in the prevailing wind direction (54 T and 234 T), which is largely influenced by wind speed and wind direction, is presented in Fig. 16a and Fig. 16b indicates the bending stress in the base of the turbine tower, measured using strain gauges and the MADV-DAQ system, and Fig. 16b indicates the corresponding strain measured in the raft of the foundation using the VWSGs and commercial DAQ system. For brevity, only an arbitrary ten days of measurements are considered during which the turbine was in operation. The results were in agreement with measurements acquired by the commercial VWSG installed in the foundation of the turbine in the same direction. Similar to the format used for labelling the strain gauges in die tower, the location of the VWSG in the raft (*R*), positioned at the top (*T*) of the raft, in a radial (*Ra*) direction, with the numerical value indicating its position relative to North. Corresponding wind speed and wind direction is indicated in Fig. 16c, remaining in-phase with the strain measurements associated with the turbine tower.

Fig. 17a and Fig. 17b indicates the bending stress in the turbine tower and corresponding strain in one of the piles in the prevailing wind direction for the period of turbine installation (Fig. 17a) and turbine operation (Fig. 17b), with bending stress in the tower measured using the MADV-DAQ system. As expected, for the period turbine installation, the bending stress in the tower was close to zero, as no wind is acting on the turbine structure. Stain measurements in the pile indicated a slight increase as a result of the turbine installation process (Fig. 15). Comparing the bending stress in the tower to the strain in the pile during turbine operation, a significant difference can be observed, with the impact of the large bending moments imposed by the wind clearly visible on both the tower and the pile. Strain results in the pile was also in-phase with the bending stress in the turbine tower and was dependent on the wind speed and wind direction. The developed MADV-DAQ system proved valuable in measuring strains and corresponding stresses in wind turbine towers, allowing for the true magnitude of the loads being transferred to the underlying foundation to be quantified.

Based on the experimental results and experience gained from the validation and field testing, the following capabilities and limitations of the MADV-DAQ are summarized:

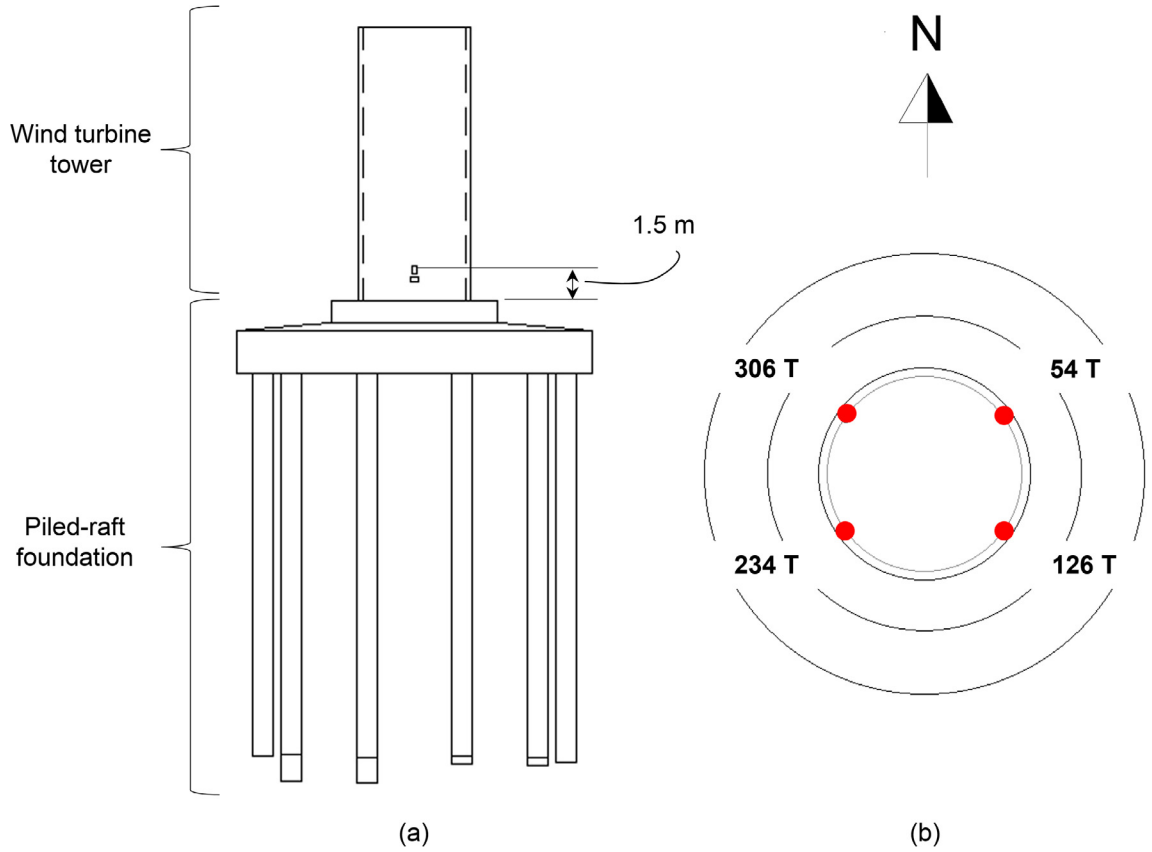

Fig. 14. Strain gauge installation positioning: (a) elevation and (b) plan view of the foundation and turbine tower.

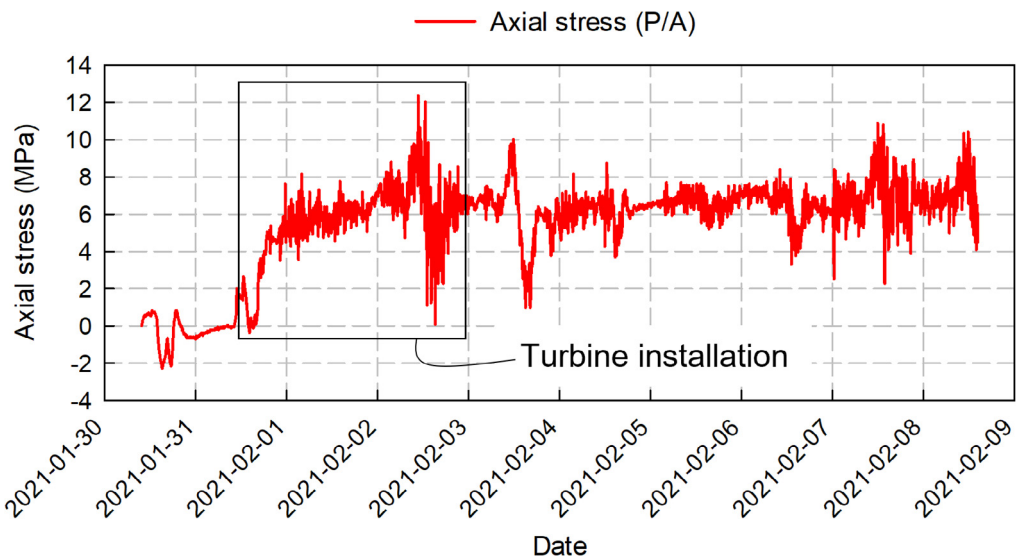

Fig. 15. Axial stress measurement (MADV-DAQ) during the installation process of the turbine.

- Compatible with any Wheatstone bridge-based sensor design, including tensiometers, strain gauges and similar MEMS-based sensors.
- Selective powering of sensors significantly reduces power consumption and self-heating of strain gauges.

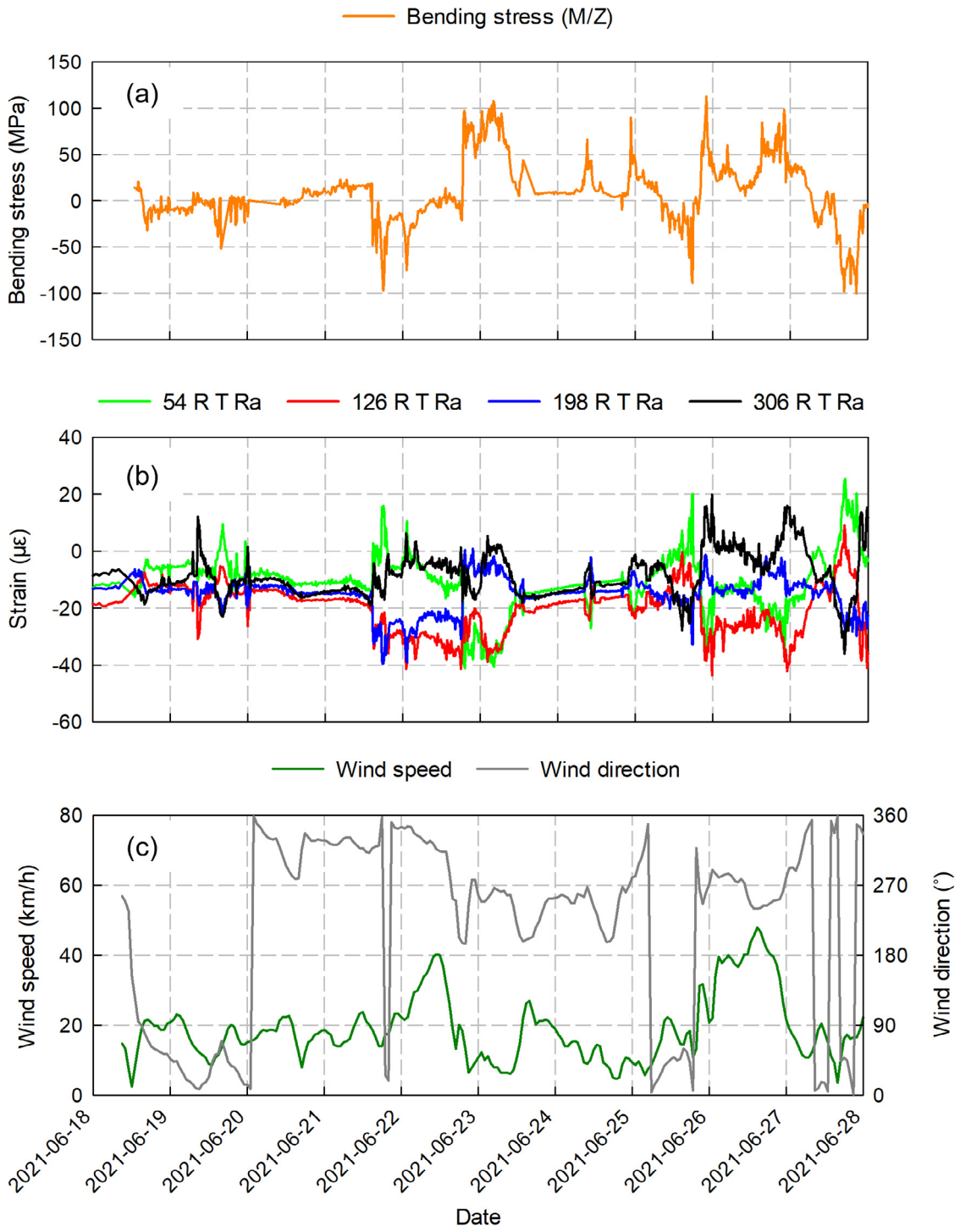

Fig. 16. Measurements: (a) bending stress (MADV-DAQ); (b) commercial VWSG and DAQs; (c) wind speed and direction (local weather station).

- The ADCs support high resolution sampling that is ideal for SHM applications.
- It remains time consuming to fabricate Veroboard-based designs and expensive to scale for small quantities if additional DAQs are desired.
- Loadshedding (rolling blackouts) negatively affected the cellular coverage with intermittent power supplied to networking equipment in the vicinity; internet connectivity is dependent on cellular coverage and power for the 4G router.

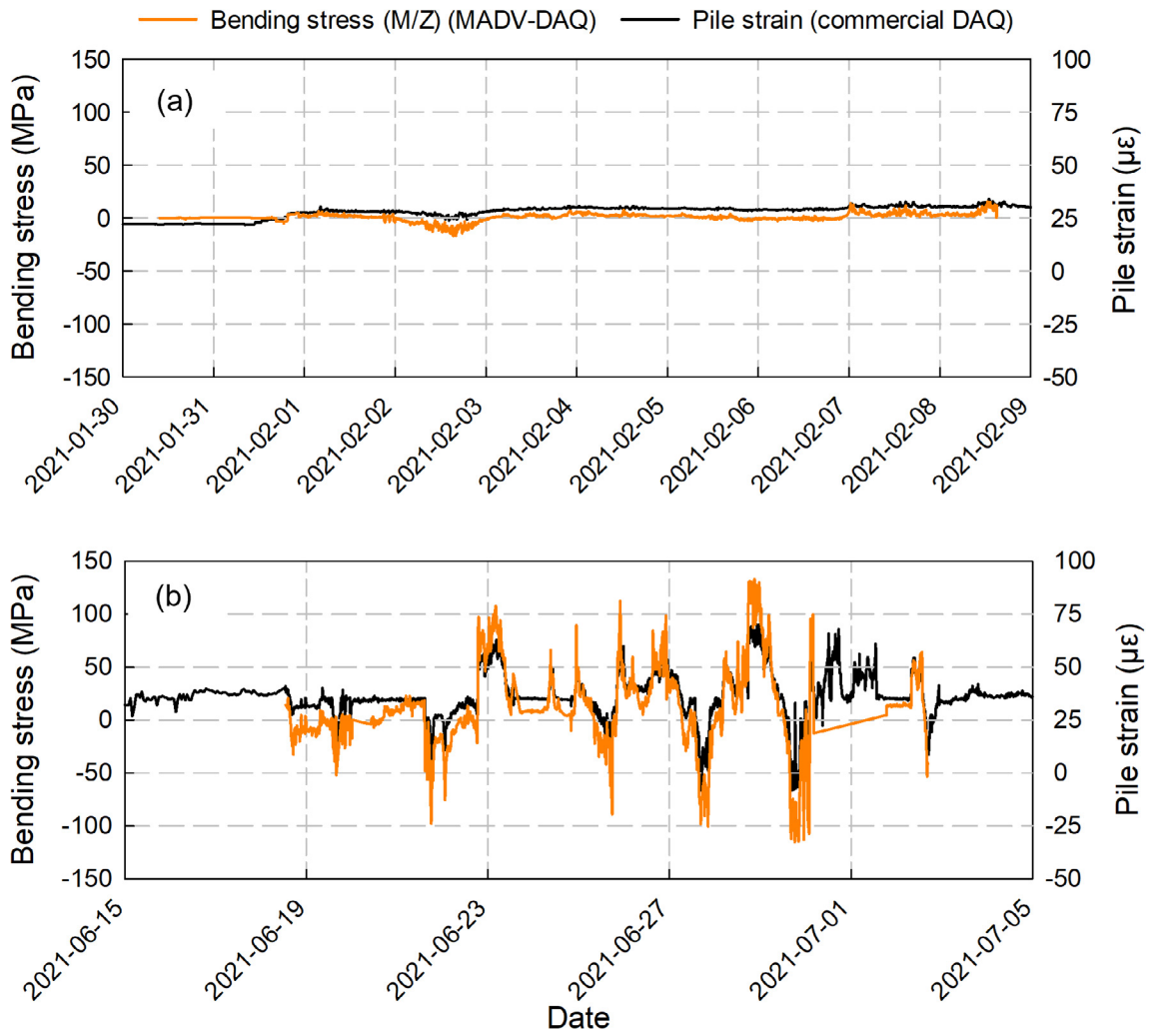

Fig. 17. Measurements comparing MADV-DAQ against the commercial DAQ: (a) turbine installation and (b) turbine operation.

- The design is limited to a full Wheatstone bridge configuration. Half- and quarter bridge configurations require additional passive resistors as a separate in-line module.
- Over-the-air (OTA) updates of updated microcontroller firmware is not supported. The new generation of Arduino [30] MKR microcontrollers does provide support for OTA updates.
- The 5 V power supply is not multiplexed for the individual sensor channels. In the (unlikely) event that a short to the ground potential occurs, no reliable or accurate strain measurements would be measured. In practice, strain gauges are more prone to tears and open connections than shorts that does not negatively affect the performance.
- The sampling frequency, full-scale and resolution is hardcoded in the firmware. Configuration over the serial connection or basic input controls would accommodate a wider range of applications and measurement requirements.

CRediT authorship contribution statement

Hendrik Louw: Conceptualization, Methodology, Validation, Formal analysis, Investigation, Data curation, Writing – original draft, Visualization, Project administration. **André Broekman:** Conceptualization, Methodology, Software, Validation, Data curation, Writing – original draft, Visualization. **Elsabé Kearsley:** Methodology, Validation, Resources, Writing – review & editing, Supervision, Project administration, Funding acquisition.

Declaration of Competing Interest

The authors declare that they have no known competing financial interests or personal relationships that could have appeared to influence the work reported in this paper.

Acknowledgements

The financial support of The Concrete Institute and the University of Pretoria is greatly acknowledged.

References

[1] E. Kearsley, S.W. Jacobsz, M.G. Alexander, H. Beushausen, F. Dehn, P. Moyo, Condition assessment of reinforced concrete beams – comparing digital image analysis with optic fibre Bragg gratings, MATEC Web Conf. 199 (2018) 06011.
[2] I. Tudosa, F. Picariello, E. Balestrieri, D.L. Carnì, F. Lamonaca, A flexible DAQ hardware architecture using SoCs for IoT based structural health monitoring systems, 2019 II Workshop on Metrology for Industry 4.0 and IoT (MetroInd4.0&IoT) (2019) 291-295. doi: 10.1109/METROI4.2019.8792900.
[3] A. Broekman, W.J.vdM. Steyn, Digital Twinning of lap-based marathon infrastructure, 2021 Rapid Product Development Association of South Africa - Robotics and Mechatronics – Pattern Recognition Association of South Africa (RAPDASA-RobMech-PRASA) (2021). doi: 10.1109/RAPDASA-RobMech-PRAS53819.2021.9829051.
[4] R.A. Swartz, J.P. Lynch, S. Zerbst, B. Sweetman, R. Rolfes, Structural monitoring of wind turbines using wireless sensor networks, Smart Struct. Systems 16 (3) (2010) 183–196, https://doi.org/10.12989/sss.2010.6.3.183.
[5] M. Currie, M. Saafi, C. Tachtatzis, F. Quail, Structural integrity monitoring of onshore wind turbine concrete foundations, Renewable Energy 83 (2015) 1131–1138, https://doi.org/10.1016/j.renene.2015.05.006.
[6] J. McAlorum, M. Perry, G. Fusiek, P. Niewczas, I. McKeeman, T. Rubert, Deterioration of cracks in onshore wind turbine foundations, Eng. Struct. 167 (2018) 121–131, https://doi.org/10.1016/j.engstruct.2018.04.003.
[7] X. Bai, M. He, R. Ma, D. Huang, Structural condition monitoring of wind turbine foundations, Energy 170 (3) (2017) 116–134, https://doi.org/10.1680/jener.16.00012.
[8] M. He, X. Bai, R. Ma, D. Huang, Structural monitoring of an onshore wind turbine foundation using strain sensors, Struct. Infrastruct. Eng. 15 (3) (2019) 314–333, https://doi.org/10.1080/15732479.2018.1546325.
[9] J.A. Basson, A. Broekman, S.W. Jacobsz, TD-DAQ: a low-cost data acquisition system monitoring the unsaturated pore pressure regime in tailings dams, HardwareX 10 (2021) e00221.
[10] A. Broekman, P.J. Gräbe, A low-cost, mobile real-time kinematic geolocation service for engineering and research applications, HardwareX 10 (2021) e00203.
[11] A. Broekman, S.W. Jacobsz, H. Louw, E. Kearsley, T. Gaspar, T.S. Da Silva Burke, Fly-by-Pi: Open source closed-loop control for geotechnical centrifuge testing applications, HardwareX 8 (2020) e00151.
[12] University of Pretoria, Engineering 4.0. https://www.up.ac.za/eng4, 2022 (accessed 27.5.2022).
[13] W.J.vdM. Steyn, A. Broekman, Civiltronics: Fusing Civil and elecTronics Engineering in the 4IR Era, SAICE Mag, Jan/Feb, 2020.
[14] Scoop, Internet of Things for Engineering 4.0 – The LoRaWAN catalyst powered by Scoop. https://scoop.co.za/blog/internet-of-things-mikrotik-lorawan, 2020 (accessed 27.5.2022).
[15] SigFox, SigFox a 0G Network. https://www.sigfox.com/, 2022 (accessed 27.5.2022).
[16] LoRa Alliance, Long Range Wide Area Network. https://www.lora-alliance.org/, 2022(accessed 27.5.2022).
[17] DFRobot, MCP3424 ADC, https://wiki.dfrobot.com/MCP3424_18-Bit_ADC-4_Channel_with_Programmable_Gain_Amplifier__SKU_DFR0316_, 2022 (accessed 27.5.2022).
[18] ExpressPCB, ExpressPCB. https://www.expresspcb.com/, 2022 (accessed 27.5.2022).
[19] SparkFun, SparkFun Thing Plus - SAMD51, https://www.sparkfun.com/products/14713,2022 (accessed 27.5.2022).
[20] Arduino, Downloads. https://www.arduino.cc/en/software, 2022 (accessed 27.5.2022).
[21] SparkFun, SparkFun Environmental Combo Breakout - CCS811/BME280 (Qwiic). https://www.sparkfun.com/products/14348, 2022 (accessed 27.5.2022).
[22] SparkFun, UV Light Sensor Breakout - VEML6075 (Qwiic). https://www.sparkfun.com/products/15089, 2022 (accessed 27.5.2022).
[23] SparkFun, SparkFun Real Time Clock Module - RV-1805 (Qwiic). https://www.sparkfun.com/products/14558, 2022 (accessed 27.5.2022).
[24] DIY-Fever, DIY Layout Creator. http://diy-fever.com/software/diylc/, 2022 (accessed 27.5.2022).
[25] Raspberry Pi Foundation, Raspberry Pi OS. https://www.raspberrypi.com/software/, 2022 (accessed 27.5.2022).
[26] PiTunnel, Access your Raspberry Pi from anywhere. https://www.pitunnel.com/, 2022 (accessed 27.5.2022).
[27] W.J.vdM. Steyn, A. Broekman, Development of a Digital Twin of a local road network: a case study, Journal of Testing and Evaluation 50(6) (2021). doi: 10.1520/JTE20210043.
[28] WUnderground, Weather Underground. https://www.wunderground.com/dashboard/pws/IEASTL7, 2022 (accessed 27.5.2022).
[29] OpenWeatherMap, OpenWeather. https://openweathermap.org/city/964432, 2022 (accessed 27.5.2022).
[30] Arduino, MKR Family. https://www.arduino.cc/pro/hardware/product-family/mkr-family?id=1996559, 2022 (accessed 27.5.2022).

Hendrik Louw is a full-time doctoral researcher and assistant lecturer in the Department of Civil Engineering at the University of Pretoria. He completed his undergraduate BEng Civil Engineering degree, BEng Hons Structural Engineering degree and MEng Structural Engineering degree from the same institution. Although involved with various research projects at the university, his main research focuses on soil-structure interaction problems related to piling and piled foundations. For his PhD research, under the supervision of Prof Elsabe Kearsley, he has instrumented and is currently monitoring the strains present in an onshore wind turbine tower and its supporting reinforced-concrete foundation under normal operating conditions. The instrumented wind turbine is part of a new wind farm in South Africa.

André Broekman is full-time PhD student and researcher in the Civil Engineering Department at the University of Pretoria, South Africa. In 2018 he obtained his MEng degree in Transportation Engineering (cum laude) under supervision of Prof. Hannes Gräbe, having graduated with a BEng Hons. Transportation degree (cum laude) in 2017 and a BEng Civil Engineering degree (cum laude) in 2016 at the University of Pretoria. He is also responsible for lecturing undergraduate students in the field of instrumentation design and assists with the development of new instrumentation hardware and software architectures for a variety of undergraduate and post-graduate research projects, collectively referred to as Civiltronics.

Elsabe Kearsley is Professor in the Department of Civil Engineering of the Engineering, Built Environment and Information Technology (EBIT) Faculty at the University of Pretoria. She holds a PhD from the University of Leeds. She worked as a Structural Design Engineering in both South Africa and the UK before becoming a staff member at the University of Pretoria. She is a registered Professional Engineer with the Engineering Council of South Africa (ECSA) and was the 2009 President of the South African Institution of Civil Engineering (SAICE) as well as the 2021/2022 President of the South African Academy of Engineering (SAAE). For the last 26 years she has been involved with cement and concrete materials research and her current research is aimed at reducing the environmental impact of cement and concrete products.